Multi-objective dynamic detection of seeds based on machine vision*

XUN Yi[1], ZHANG Junxiong[1], LI Wei[1]** and CAI Weiguo[2]

(1. College of Engineering, China Agricultural University, Beijing 100083, China; 2. College of Science, Dalian Fisheries University, Dalian 116023, China)

Accepted on August 8, 2006

Abstract An approach to inspecting massive numbers of moving seeds was studied based on the techniques of dynamic inspection and machine vision. A progressive scanning CCD camera with external trigger function was used for real-time capture of dynamic images of seeds. The methods based on R channel of RGB (Red, Green and Blue) and region-dependent segmentation were adopted to reduce the data size of image processing and improve the efficiency of seeds inspection. All the seeds were sorted into four grades according to their morphological characteristics, such as surface area, perimeter, major axis, minor axis, circularity and eccentricity. The detection experiments indicated that the eligible ratio of the classifications was about 81.90% by this real-time inspection system.

Keywords: machine vision, seed sorting, multi-objective, morphological parameter.

Purity, health, consistency, etc. are main criteria in the seeds refined separating standards published by the International Seed Testing Association (ISTA). In some countries seeds were exactly inspected and sorted one by one or in a small batch. The sorted seeds through such processes have high consistency at quality, shape and color, and their germination rate is greatly improved. They are especially suitable for precise quantity sowing and mechanized operation, which can reduce planting costs and improve agricultural automation level.

The main operation of a traditional seeds quality inspection is seeds cleaning that is prone to a mechanical damage to seeds, which leads to a low product quality. However, the inspection by machine vision provides a faster and non-destructive approach compared to the traditional sizing equipment currently used in seed industry. Machine vision has been used to inspect and grade various grain types including wheat[1–3], rice[4–6], corn[7] and lentils. Using image processing and neural network, Wang et al.[8] determined vitreous wheat with reasonably high accuracy. Shahin[9] studied the lentil seed size distribution with machine vision. Cogdill[10] analyzed the single-kernel maize by near-infrared hyper-spectra imaging. In most of the aforementioned applications, seeds were manually placed on a plate or tray under the controlled conditions in laboratories and such processes cannot be adopted for on-line inspections. Wan[11,12] developed an automatic grain quality inspection system which basically realized automatic feeding and grain grading. However, the conveyor belt must be temporarily stopped to take photograph of grain kernel images by a camera. The efficiency for grain inspection decreased.

In this work the methods for image grabbing of massive numbers of seeds and image analysis were studied based on our prior work of a self-developed precise seeds grading test-bed[13]. The effective seed characteristic information from the image of fast moving seeds was extracted and an on-line seeds grading process was realized.

1 Automatic inspection system

The structure of seeds grading test-bed is shown in Fig. 1. The feeding device was installed on the right of the inspection line. The conveyor belt was driven by a motor and moved at a uniform speed. By using the feeding device, the corn kernels were scattered over the conveyor belt. With the help of a scrape brush and a spin brush, the corn kernels were swept into the prefabricated holes on the conveyor belt separately.

Some images of corn kernels were taken by a CCD camera connected with the computer of the image processing unit when the kernels passed through the image acquisition unit. The computer segregated

* Supported by National Natural Science Foundation of China (Grant No. 30471011)

** To whom correspondence should be addressed. E-mail: gxy5@cau.deu.cn

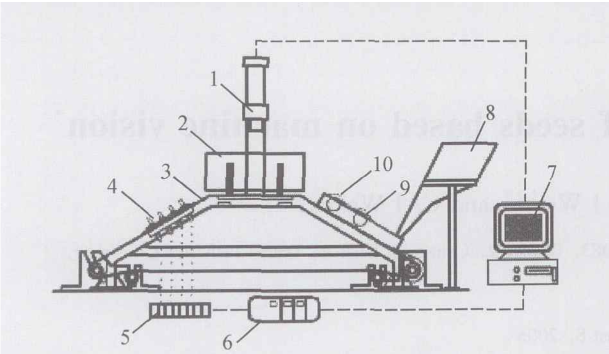

Fig. 1. The structure of seeds grading test-bed. 1, CCD camera; 2, light sources; 3, conveyer belt; 4, guide tubes; 5, magnet valves; 6, PLC; 7, images; 8, feeding device; 9, scrape brush; 10, spin brush.

the kernels from the background in the images, analyzed the signals by a recognition process, and transmitted the final sorting results to a PLC. In the discharging section, the controller signaled to each corresponding pneumatic magnet valve to eject the kernels from the carrying holes into collection containers. An interface protocol between the inspection machine and the image processing unit was developed to coordinate their concurrent activity. The system completed seeds discharging, grading and collecting operations. At the same time, it controlled conveyor belt speed, color code sensors, grading device and counter.

2 Real-time images grabbing of moving seeds

A progressive scanning CCD camera (Join Hope AC1300) and an image board (Join Hope RGB10B) were used to capture the entire image at one time. Illumination was provided by eight 15 W fluorescent lights. They were symmetrically placed on two white boards to produce a uniform illumination across the entire field of view. Images were taken on a black conveyor belt, which could be easily segmented by standard segmentation routines because of the color difference versus the seeds.

To grab an image exactly, an external trigger function of the CCD camera was used and controlled by color code sensors and the PLC. There were three color code sensors in the system and their installation positions were shown in Fig. 2.

The color code sensors played different roles when the conveyor belt was moving. The first sensor sent signal for photographing the first image, and turned the third sensor at the same time. When the first sensor detected the color code signal, the camera was triggered and the first photograph was taken. When the second sensor detected the color code signal, it indicated that the seeds had entered into the grading section and then the seeds positions were real-time tracked by the third sensor. A picture would be photographed after each four color codes were induced by the third sensor. Fig. 3 shows the images real-time captured.

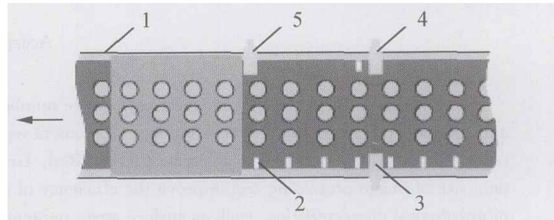

Fig. 2. The installation positions of color code sensors. 1, Conveyor belt; 2, color code; 3, code sensor 3; 4, code sensor 1; 5, code sensor 2.

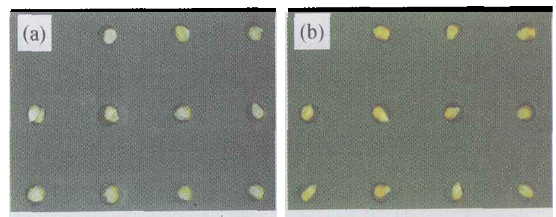

Fig. 3. Corn kernels images. (a) NongDa-3138; (b) NongDa-4967.

3 Seeds images identification and processing

3.1 Images pre-treatment

The seeds of NongDa-3138, NongDa-108, and NongDa-4967 (three novel varieties of corn seed developed by China Agricultural University) were taken as research objectives. The seeds were spread onto the conveyor belt. As shown in Fig. 4, the images were obtained in real-time inspection and their effective pixels resolution was 788(H) × 576(V). A working distance of 750 mm was transformed into a resolution of 1 pixel = 0.185 mm (along scanning line). The images were analyzed and the following features were concluded: 1) The seeds positions remained almost unchanged in all images; 2) with the help of the scrape brush and the spin brush, most of the seeds moved upward or downward; 3) some holes of conveyor belt probably had two seeds kernels or nothing; 4) the effective data accounted for 32.82% of all data only for an image; 5) the images had a good consistency. According to the above features, the whole image was divided into 12 independent regions using the method of region-dependent segmentation.

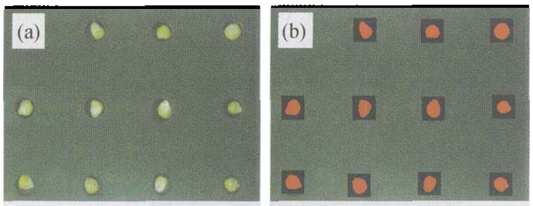

Fig. 4. Corn kernels image pre-processing. (a) Original image; (b) pre-processed image.

To reduce the data size needed in image processing, the paper adopted a method based on R (Red) channel of RGB (Red, Green, and Blue). In R channel the difference between grey level average of the background and that of the seeds is relatively great. It is easy to separate each seed from its background.

The concrete steps for calculating the size of every region were as follows: 1) The original image was divided into 12 independent rectangular windows with size of 100×100 pixels; 2) the image data of R channel was copied to a new memory field; 3) the targets were separated from background through a fixed threshold value; 4) the pixels numbers A and centroid of each target were calculated. If the value of A was less than 500, then there was no seed in this region; otherwise, 12 new windows (black areas in Fig. 4(b)) were made and each of them had a size of 70×70 pixels with superposition of its geometric center and the centroid of each target. Image processing and pattern recognition would be completed in these regions. In this way, a region labeling was not needed and the data size of image processing was reduced to 13.29% of the original. The influence of image noise on the calculating morphological parameters was also decreased.

In each region with seed, a fast median filtering algorithm was used to eliminate noise on the image and then the threshold method was used to separate each seed from its background. An image containing 12 matrix-positioned corn kernels was processed to obtain each kernel image for parameters calculation. Fig. 4(b) is a pre-processed image.

3.2 Morphological parameters extraction

Seeds morphological parameters can be classified into two groups: the basic parameters and the derived parameters.

The basic parameters include:

Area (A)—area of a kernel measured as the number of pixels in polygon;

perimeter (P)—the mathematical sum of the Euclidean distance between all the successive pairs of pixel around the circumference of the kernel;

major axis length (L)—the longest line that can be drawn through the object;

minor axis length (l)—the longest line that can be drawn through the object perpendicular to the major axis.

The derived parameters include:

Circularity—it describes the compactness of the region and given by

$$C = (4\pi A)/P^2; \quad (1)$$

eccentricity—it describes the shape of the region and given by

$$e = L/l; \quad (2)$$

α—it is given by

$$\alpha = l_{max}/l_{min}, \quad (3)$$

where l_{max} and l_{min} are the maximum and minimum Euclidean distances between central point and every boundary point, respectively.

The morphological parameters were obtained by on-line inspection using the calculation functions developed in C++ code. Table 1 shows a part of comparison between on-line measured results and those of human measured from over 800 randomly sampled corn kernels. The average measuring errors were 0.231 mm and 0.211 mm for the major axis length and minor axis length, respectively.

Table 1. Consistency between machine and human measure

No	Machine measure		Human measure	
	L(mm)	l(mm)	L(mm)	l(mm)
1	7.59	5.92	7.48	5.70
2	9.07	6.66	8.80	6.88
3	11.47	9.07	11.30	9.26
4	8.14	7.03	7.20	6.76
5	7.59	7.03	7.24	6.40
6	9.81	7.40	9.54	7.68
7	9.44	8.14	9.50	8.80
8	8.69	6.48	8.64	6.20
9	9.44	8.33	9.90	8.00
10	10.36	7.59	9.50	8.80
11	9.83	8.46	9.71	8.23
12	10.78	8.67	10.59	8.53
13	7.76	5.67	7.70	5.59
14	11.84	9.12	11.60	8.92
…	…	…	…	…

3.3 Overlapping seeds identification

According to the analysis of the images, an unavoidable fact is that two kernels enter into one hole, which will affect the inspection accuracy and cause difficulties in ejecting the kernels from the carrying holes into collection containers. Considering the overlapping of two seeds as a whole body, its figure is similar to that of Arabic numeral "8" and its centroid is approximately located on the junction of the two kernels, as shown in Fig. 5. $d_{\min}$ is the minimum value of Euclidean distance between centroid and every boundary point. The minimum $d_{\min}$ for the whole body is smaller and L (the major axis length) is larger than that of the single one. So the ratio of L to $d_{\min}$ is a relatively large value. Using statistical methods, the seeds would not be processed later and entered into containers prepared beforehand if the ratio of L to $d_{\min}$ is greater than 3.5, in case of which there may be two kernels in a hole.

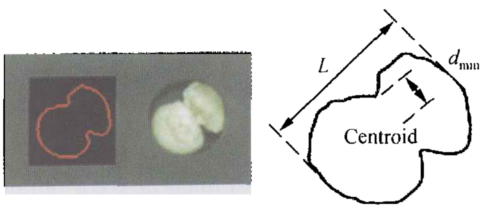

Fig. 5. Contour of overlapping seeds.

4 Method of seeds grading

In the growth period of corn seeds, their absorption ability for nutrition varies with different locations of the grain ear. Their size, shape and size of endosperm are different. As shown in Fig. 6, corn seed kernels were sorted into 4 grades (large-flat, large-round, small-flat and small-round) according to an international practice. After grading, the seeds with the same grade come from the same part of the grain ear, their shape, size, germination energy and size of endosperm are similar, and their genetic characters are basically coincident.

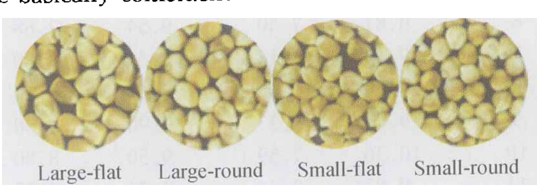

Fig. 6. Corn kernels of different grades.

Through the comparison of the contours between flat-seeds and round-seeds, the figures of most flat-seeds are slender, while those of most round-seeds are round, as shown in Fig. 7.

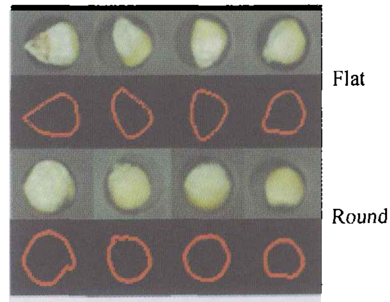

Fig. 7. Figure and contour of corn kernels.

By means of statistics analysis, three morphological parameters are propitious to distinguish flat-seed and round-seed in NongDa-4967 inspection. They are eccentricity, circularity and α, and the sequence of their adaptabilities is eccentricity, α and circularity.

There were four steps for sorting the seeds: 1) Classifying all seeds into three portions according to seeds areas. The seeds with areas over 1538 pixels were large-flat and large-round; those areas below 1449 pixels were small-round and small-flat; and the others were large-round and small-flat. 2) For each portion, seeds were identified according to eccentricity. 3) Some seeds which could not be classified by eccentricity were identified according to α. 4) The others were detected according to circularity. So far, all the seeds were sorted into four grades.

5 Tests results and analysis

A small batch of seeds (NongDa-4967) were selected randomly and sorted manually into four grades. Each grade had two hundred kernels. The seeds of each grade were processed by the automatic inspection system. Table 2 shows the on-line inspection results of NongDa-4967. At a certain conveyer belt speed, the operation was repeated for 15 times.

In Table 2, N_1, N_2, N_3 and N_4 are the average number of kernels that are ejected into the corresponding containers. R_1, R_2, R_3 and R_4 are the average eligible grading ratio of the corresponding grade, respectively. R_i is defined by

$$R_i = N_i/200 \quad (i = 0, \cdots, 4). \tag{4}$$

R_s is the average of the eligible grading ratio of the four grades and defined by

$$R_s = \frac{1}{4}\sum_{i=0}^{4} R_i. \tag{5}$$

Table 2. On-line inspection results of NongDa-4967

Conveyer belt speed (m/s)	Large-flat		Large-round		Small-flat		Small-round		R_s(%)
	N_1	R_1(%)	N_2	R_2(%)	N_3	R_3(%)	N_4	R_4(%)	
0.10	162	81.0	160	80.0	169	84.5	167	83.5	82.3
0.15	168	84.0	172	86.0	170	85.0	173	86.5	85.4
0.20	172	86.0	170	85.0	174	87.0	176	88.0	86.5
0.25	160	80.0	165	82.5	170	85.0	171	85.5	83.3
0.30	154	77.0	159	79.5	157	78.5	160	80.0	78.8
0.35	152	76.0	149	74.5	148	74.0	152	76.0	75.1

The same approach can be applied to other speeds. The average eligible grading ratio of the system is 81.90% by calculating the average of these results.

When the belt speed was 0.3 m/s, the time-interval of capturing an image was 400 ms. These images were acquired, processed by a Pentium 2.6 GHz computer, equipped with 512 M of memory. The process time for an image containing 12 corn seeds was 60 ms. The less seeds an image had, the less time the process needed. The process time for an image without a seed was only 40 ms. It satisfied real-time inspection.

The eligible grading ratio will decrease when the belt speed is more than 0.2 m/s. With the increasing belt speed, the opening time of the magnet valves will be shorter and less gas will be exhausted, which results in increased defeated blow seeds and a decreased eligible grading ratio.

6 Conclusion

An on-line machine vision based seeds grading system was realized. An image acquisition system, composed of a progressive scanning CCD camera with external trigger function, an image board, PLC, color code sensors and a computer, was utilized to capture distinct moving seeds images. The methods based on R channel of RGB and region-dependent segmentation were adopted to reduce the data size of image processing and to improve the efficiency for seeds inspection. Corn seeds of NongDa-3138, NongDa-108, and NongDa-4967 were sorted into four grades according to their morphological parameters with the system. The experimental results showed that the average eligible grading ratio of the system was 81.90%.

References

1 Zayas I., Lai F. S. and Pomeranz Y. Discrimination between wheat classes and varieties by image analysis. Cereal Chemistry, 1986, 63(1): 52—56.

2 Zayas I., Pomeranz Y. and Lai F. S. Discrimination of wheat and non-wheat components in grain samples by image analysis. Cereal Chemistry, 1989, 63(3): 233—237.

3 Haff R. F. and Slaughter D. C. X-ray inspection of wheat for granary weevils. In: ASAE Annual International Meeting. Toronto, Canada, July, July 18—21, 1999, ASAE Paper No. 99—3060.

4 Melvin S., Karunakaran C., Jayas D. S. et al. Design and development of a grain kernel singulation device. Canadian Biosystems Engineering, 2003, 45: 31—33.

5 Jayas D. S., karunakaran C. and Paliwal J. Grain quality monitoring using machine vision and soft x-rays for cereal grains. http://pasture.ecn.purdue.edu/~grainlab/IQGC1/proc/pdf/jayas.pdf [2004-07-20]

6 Kawamura S., Natsuga M., Takekura K. et al. Development of an automatic rice-quality inspection system. Computers and Electronics in Agriculture, 2003, 40(2): 115—126.

7 Ni B., Paulsen M. R. and Reid J. F. Size grading of corn kernels with machine vision. Applied Engineering in Agriculture, 1998, 14(5): 567—571.

8 Wang N., Dowell F. E. and Zhang N. Q. Determining wheat vitreousness using image processing and a neural network. Transactions of the ASAE, 2003, 46(4): 1143—1150.

9 Shahin M. A. and Symons S. J. Lentil seed size distribution with machine vision. In: ASAE Annual International Meeting. California, USA, July 30-August 1, 2001, ASAE Paper No. 01—3058.

10 Cogdill R. P., Hurburgh C. R. and Rippke G. R. Single-kernel maize analysis by near-infrared hyperspectra imaging. Transactions of the ASAE, 2004, 47(1): 311—320.

11 Wan Y. N. The study of brown rice quality grading with an automated quality inspection machine. In: ASAE Annual International Meeting. Toronto, Canada, July, July 18—21, 1999, ASAE Paper No. 99—3196.

12 Wan Y. N. The design of an automatic grain quality inspection system. In: ASAE Annual International Meeting. Toronto, Canada, July, July 18—21, 1999, ASAE Paper No. 99—3200.

13 Cai W. G., Li W. and Xun Y. Study on automatic control method of seeds grading device. Transactions of the Chinese Society for Agricultural Machinery (in Chinese), 2005, 36(8): 90—92.